

## ARTICLE

# Potassium homeostasis and therapeutic intervention with sodium zirconium cyclosilicate: A model-informed drug development case study

Lindsay E. Clegg<sup>1</sup>  | Lulu Chu<sup>2</sup> | Mats Nagard<sup>1</sup>  | David W. Boulton<sup>1</sup>  | Robert C. Penland<sup>2</sup> 

<sup>1</sup>Clinical Pharmacology and Quantitative Pharmacology, Clinical Pharmacology and Safety Sciences, R&D, AstraZeneca, Gaithersburg, Maryland, USA

<sup>2</sup>Clinical Pharmacology and Quantitative Pharmacology, Clinical Pharmacology and Safety Sciences, R&D, AstraZeneca, Waltham, Massachusetts, USA

**Correspondence**

Lindsay E. Clegg, 1 Medimmune Way, Gaithersburg, MD 20878, USA.  
Email: [lindsay.clegg1@astrazeneca.com](mailto:lindsay.clegg1@astrazeneca.com)

**Present address**

Lulu Chu, Takeda Pharmaceuticals U.S.A., Inc., Lexington, Massachusetts, USA

**Abstract**

Potassium ( $K^+$ ) is the main intracellular cation in the body. Elevated  $K^+$  levels (hyperkalemia) increase the risk of life-threatening arrhythmias and sudden cardiac death. However, the details of  $K^+$  homeostasis and the effects of orally administered  $K^+$  binders, such as sodium zirconium cyclosilicate (SZC), on  $K^+$  redistribution and excretion in patients remain incompletely understood. We built a fit-for-purpose systems pharmacology model to describe  $K^+$  homeostasis in hyperkalemic subjects and capture serum  $K^+$  ( $sK^+$ ) dynamics in response to acute and chronic administration of SZC. The resulting model describes  $K^+$  distribution in the gastrointestinal (GI) tract, blood, and extracellular and intracellular spaces of tissue, renal clearance of  $K^+$ , and  $K^+$ -SZC binding and excretion in the GI tract. The model, which was fit to time-course  $sK^+$  data for individual patients from two clinical trials, accounts for bolus delivery of  $K^+$  in meals and oral doses of SZC. The virtual population of patients derived from fitting the model to these trials was then modified to predict the SZC dose-response and inform clinical trial design in two new applications: emergency lowering of  $sK^+$  in severe hyperkalemia and prevention of hyperkalemia between dialysis sessions in patients with end-stage chronic kidney disease. In both cases, the model provided novel and useful insight that was borne out by the now completed clinical trials, providing a concrete case study of fit-for-purpose, model-informed drug development after initial approval of a drug.

**Study Highlights****WHAT IS THE CURRENT KNOWLEDGE ON THE TOPIC?**

While potassium ( $K^+$ ) is the primary intracellular cation in the body, and hyperkalemia can be life-threatening, no mathematical models of  $K^+$  homeostasis exist.

This is an open access article under the terms of the [Creative Commons Attribution-NonCommercial](https://creativecommons.org/licenses/by-nc/4.0/) License, which permits use, distribution and reproduction in any medium, provided the original work is properly cited and is not used for commercial purposes.

© 2023 AstraZeneca. *CPT: Pharmacometrics & Systems Pharmacology* published by Wiley Periodicals LLC on behalf of American Society for Clinical Pharmacology and Therapeutics.

### WHAT QUESTION DID THIS STUDY ADDRESS?

This analysis built a fit-for-purpose systems pharmacology model of  $K^+$  homeostasis and treatment with sodium zirconium cyclosilicate (SZC). The model was applied to design of clinical trials of SZC in emergency lowering of severe hyperkalemia, and maintenance of normokalemia in patients on hemodialysis.

### WHAT DOES THIS STUDY ADD TO OUR KNOWLEDGE?

This analysis adds to our knowledge of  $K^+$  distribution, and the effects of SZC on  $K^+$  redistribution in the body, as well as providing a concrete case study of model-informed drug development.

### HOW MIGHT THIS CHANGE DRUG DISCOVERY, DEVELOPMENT, AND/OR THERAPEUTICS?

This model demonstrates the ability of fit-for-purpose modeling to meaningfully contribute to decision making during drug development, including extrapolation to new populations and applications after the initial drug approval.

## INTRODUCTION

Potassium ( $K^+$ ) is the primary intracellular cation in the body, with ~98% of total body  $K^+$  residing intracellularly. Normal  $K^+$  intake is around 70–150 mmol/day, yet tissue extracellular and serum  $K^+$  ( $sK^+$ ) remain within the normal range of 3.5–5.0 mmol/L in healthy subjects, even when  $K^+$  intake varies from 10 to 400 mmol/day.<sup>1,2</sup> This tight regulation is critical to maintain cellular function; both hyperkalemia and hypokalemia, if severe, are life-threatening.<sup>3</sup> Normally,  $K^+$  is excreted primarily (80%–90%) via the kidneys, and is regulated by aldosterone, which increases in response to elevated  $sK^+$ , acting in the distal nephron to increase sodium reabsorption and  $K^+$  excretion.<sup>1,2,4</sup> Renal  $K^+$  excretion also follows a circadian rhythm, increasing during the day and decreasing at night (typically varying <10% over the course of the day),<sup>5</sup> even with equal-sized evenly spaced meals.<sup>5–7</sup> Gastrointestinal (GI) excretion of  $K^+$ , which accounts for the remainder of  $K^+$  clearance, increases in late-stage chronic kidney disease (CKD).<sup>8,9</sup> Insulin and beta-adrenergic tone are important regulators of  $K^+$  uptake into cells, buffering extracellular  $K^+$  levels following meals much more quickly than changes to  $K^+$  excretion.<sup>5</sup>

Chronic hyperkalemia ( $sK^+ > 5$  mmol/L) occurs most often in patients with renal disease and/or heart failure and with use of renin-angiotensin-aldosterone system inhibitors (RAASi) due to insufficient renal clearance of  $K^+$ .<sup>1</sup> Indeed, concerns about hyperkalemia contribute to suboptimal dosing of RAASi, particularly mineralocorticoid receptor antagonists.<sup>1,10,11</sup> The shift in extracellular  $K^+$  alters the transmembrane potential on cardiac myocytes and neurons, elevating risk of life-threatening cardiac arrhythmias and death.<sup>5</sup> Hyperkalemia can also occur acutely as a result of large intracellular shifts in  $K^+$  (e.g., traumatic injury or tumor lysis).

Depending upon severity, hyperkalemia is traditionally treated with a low- $K^+$  diet, reduction of RAASi dosage,

dialysis, and/or compounds that bind  $K^+$  in the GI tract,<sup>4,12</sup> such as sodium polystyrene sulfonate. More recently,  $K^+$  binders, such as patiromer and sodium zirconium cyclosilicate (SZC; previously known as ZS or ZS-9), have become available. SZC is an orally administered, inorganic crystalline material that binds in a highly specific manner to  $K^+$  in the GI tract, but is not absorbed into systemic circulation.<sup>13</sup> SZC acts by creating a gradient to pull  $K^+$  out of circulation and/or reducing absorption of  $K^+$  from the GI tract after a meal. SZC was developed for acute three times per day (t.i.d.) dosing to reduce  $sK^+$ , and then chronic once per day (q.d.) dosing to maintain normokalemia.<sup>14,15</sup> SZC has been shown to be safe and effective at reducing  $sK^+$  within 1 h of the first dose.<sup>16</sup> The reductions in  $sK^+$  observed are proportional to baseline  $K^+$  levels, leading to effective normalization of  $sK^+$  (<5.1 mM) in 98% of patients within 48 h of treatment onset, and a low incidence of hypokalemia ( $sK^+ < 3.5$  mmol/L).<sup>14</sup> However, the effects of SZC on  $K^+$  redistribution and excretion in patients are not fully understood.

Although the first mathematical models of  $K^+$  homeostasis have recently been published,<sup>17,18</sup> these models were built on population-level data in the literature. A better understanding of  $K^+$  homeostasis in individual patients within a hyperkalemic population would facilitate optimization of treatment with medications such as SZC, as well as clinical trial design and dosing regimen selection for new patient populations or indications, including quickly reducing  $sK^+$  in an emergency setting, and maintaining normokalemia between dialysis sessions in patients with end-stage CKD.

## Objectives

The objective of this work was to build a fit-for-purpose systems pharmacology model that could describe  $K^+$

homeostasis in hyperkalemic subjects, and capture  $sK^+$  dynamics in response to acute and chronic administration of SZC. The model was designed to incorporate sufficient physiological detail to effectively capture  $K^+$  dynamics and allow for extrapolation to severe hyperkalemia and hemodialysis, while maintaining as concise and understandable a model structure as possible. The resulting model, although relatively simple, has been effectively used to inform internal decision making for multiple new applications for SZC, and, as such, represents a concrete case study of model-informed drug development after initial drug approval.

## METHODS

### Model structure

The  $K^+$  homeostasis model is an open system, comprised of four compartments (Figure 1), and a set of six nonlinear coupled ordinary differential equations. The four compartments represent the main contributions to  $K^+$  homeostasis in the body: (1) the GI tract (combined stomach, small intestine, and large intestine), where SZC acts; (2) blood (plasma/serum), where  $K^+$  is most commonly measured; (3) tissue extracellular fluid; and (4) intracellular space in tissues, where ~98% of total body  $K^+$  is located. The model accounts for two-way transport of  $K^+$  between each compartment, as well as  $K^+$  removal from the GI tract in feces and from the blood via the kidneys. Renal  $K^+$  clearance is a function of estimated glomerular filtration rate (eGFR) and a diurnal variation function. SZC is not absorbed from the GI tract,<sup>16</sup> and therefore not present in the other compartments. Meals and oral doses of SZC were implemented as boluses, that is, consumed instantaneously into the lumped GI compartment; GI transit time before  $K^+$  can be absorbed or SZC can bind to  $K^+$  is not accounted for. SZC reversibly binds to  $K^+$  in the GI tract, and free or  $K^+$ -bound SZC are cleared in feces (the same rate is assumed for SZC clearance whether free or bound to  $K^+$ ).

### Model equations

The SZC- $K^+$  homeostasis model includes four differential equations to account for  $K^+$  concentrations in each compartment, including intercompartment transport,  $K^+$  intake, GI and renal  $K^+$  elimination (a combination of  $K^+$  filtration, re-absorption, and secretion), and  $K^+$  binding to SZC in the GI tract. Two additional equations describe SZC and K-SZC concentrations in the GI tract. Diurnal variation in renal clearance of  $K^+$  was accounted for by the term  $m(t)$ ; a sinusoidal variation in renal  $K^+$  clearance over the course

of a day is assumed, with maximum clearance at noon and minimum clearance at midnight.<sup>5-7</sup> The magnitude of the variation ( $p$ ) was optimized for each subject. Parameters and volumes are defined in Table 1 and Table S1, respectively.

### Potassium homeostasis

$$\frac{d[K]_{GI}}{dt} = -r_{CL,K} \cdot [K]_{GI} - r_{on}[K]_{GI} \cdot [SZC]_{GI} + r_{off}[K \cdot SZC]_{GI} - r_{GB}[K]_{GI} + r_{BG}[K]_B \cdot \frac{v_B}{v_G} + r_{in,K}(t)$$

$$\frac{d[K]_B}{dt} = -r_f \cdot [K]_B \cdot m(t) \cdot eGFR/60 + r_{GB}[K]_{GI} \cdot \frac{v_G}{v_B} - r_{BG}[K]_B + r_{EB}[K]_E \cdot \frac{v_E}{v_B} - r_{BE}[K]_B$$

$$\frac{d[K]_E}{dt} = -r_{EB}[K]_E + r_{BE}[K]_B \cdot \frac{v_B}{v_E} - r_{EI}[K]_E + r_{IE}[K]_I \cdot \frac{v_I}{v_E}$$

$$\frac{d[K]_I}{dt} = r_{EI}[K]_E \cdot \frac{v_E}{v_I} - r_{IE}[K]_I$$

$$m(t) = 1 - p \cdot \cos\left(\frac{\pi \cdot t_d}{12}\right), \text{ where } t_d \text{ is the hour in the day } [0, 24]$$

### SZC equations

$$\frac{d[SZC]_{GI}}{dt} = -r_{CL,SZC} \cdot [SZC]_{GI} - r_{on}[K]_{GI} \cdot [SZC]_{GI} + r_{off}[K \cdot SZC]_{GI} + r_{in,SZC}(t)$$

$$\frac{d[K \cdot SZC]_{GI}}{dt} = -r_{CL,SZC} \cdot [K \cdot SZC]_{GI} + r_{on}[K]_{GI} \cdot [SZC]_{GI} - r_{off}[K \cdot SZC]_{GI}$$

### Model assumptions

The model structure assumes well-mixed compartments, between which  $K^+$  is transported passively. In the model, time zero is the midnight preceding administration of the first dose of SZC. In each simulation, initial concentrations were specified based on steady-state values under constant  $K^+$  intake and no SZC treatment (Figure S1), and then the model is run for sufficient time to attain steady-state under normal  $K^+$  meal conditions before SZC dosing.

The volumes of the compartments are based on physiological scaling of water volumes, assuming volumes to be directly proportional to patient weight.<sup>19</sup> Body composition was not taken into account, as height data to calculate body mass index was unavailable. Only accessible tissue extracellular fluid was considered, excluding water in

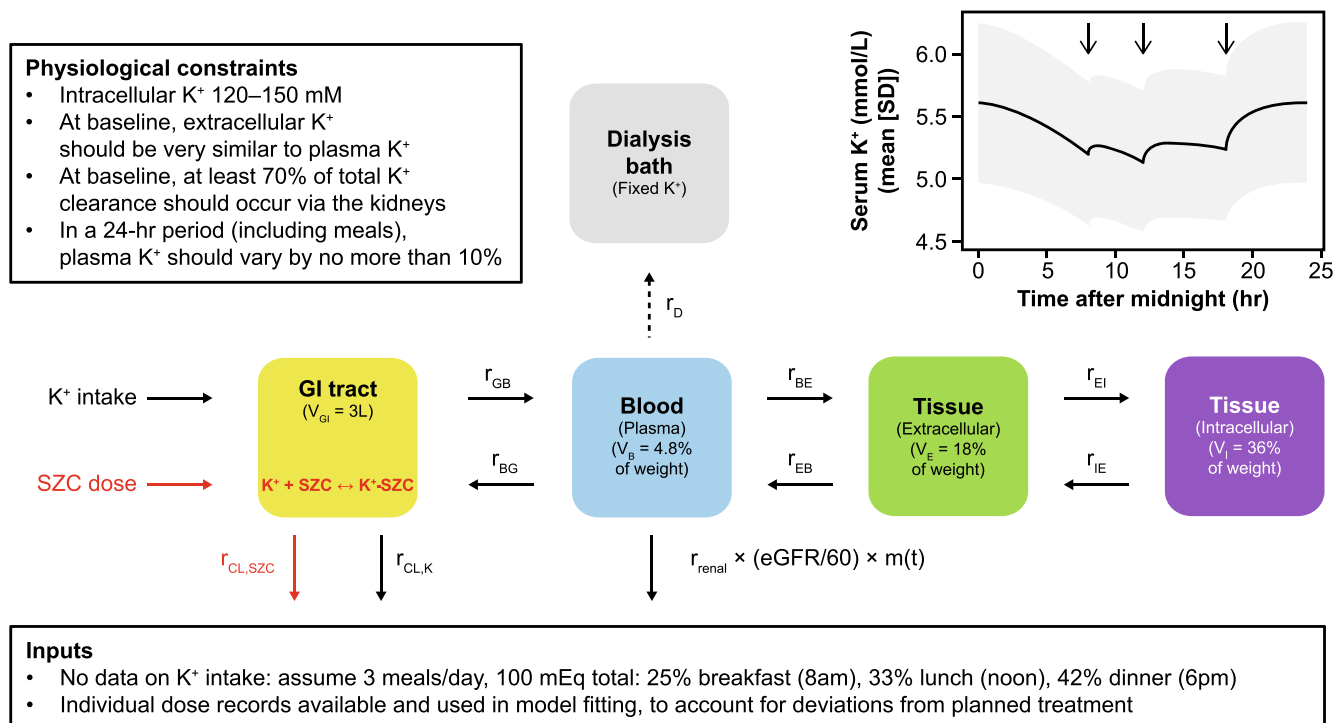


**FIGURE 1** Model overview. Main: schematic of model compartments and parameters, including the “dialysis bath” compartment added to the model for the hemodialysis application. Top left inset: literature-based physiological constraints imposed to ensure reasonable model behavior.<sup>19</sup> Top right inset: daily variability in  $sK^+$  in the virtual population in the absence of SZC treatment. Arrows represent meals. Time zero is midnight. The line is the mean and the shaded band is the mean  $\pm$  SD. Bottom inset: Details of assumed  $K^+$  consumption and patient-specific SZC dosing. eGFR, estimated glomerular filtration rate; GI, gastrointestinal;  $K^+$ , potassium;  $r_{BE}$ ,  $K^+$  transport blood to tissue extracellular fluid;  $r_{BG}$ ,  $K^+$  transport blood to GI;  $r_{CL,K}$ ,  $K^+$  clearance, GI (feces);  $r_{CL,SZC}$ , SZC and  $K^+$ -SZC clearance, GI (feces);  $r_D$ , rate of  $K^+$  transfer;  $r_{EB}$ ,  $K^+$  transport tissue extracellular fluid to blood;  $r_{EI}$ ,  $K^+$  uptake by cells in tissue;  $r_{GB}$ ,  $K^+$  transport GI to blood;  $r_{IE}$ ,  $K^+$  release by cells in tissue;  $r_{renal}$ , renal  $K^+$  clearance from blood;  $m(t)$ , diurnal variation in renal clearance of  $K^+$ ; SD, standard deviation;  $sK^+$ , serum potassium; SZC, sodium zirconium cyclosilicate;  $V_b$ , volume of blood compartment;  $V_e$ , volume of extracellular compartment;  $V_{GI}$ , volume of gastrointestinal tract;  $V_i$ , volume of intracellular compartment.

bone and dense connective tissue that equilibrates slowly with the main bulk of tissue extracellular fluid.<sup>19</sup> It was assumed that GI tract volume does not scale with body weight, and was fixed at 3 L, accounting for the stomach, small intestine, and large intestine,<sup>20,21</sup> although the bulk of SZC  $K^+$ -binding likely occurs in the small intestine.<sup>13</sup> Compartment volumes are given in Figure 1, and the derivations are summarized in Table S1.

Note that, due to the model structure, after cessation of dosing with SZC, all simulated subjects return (over the course of days) to their baseline hyperkalemic state. Thus, this model is better suited to capture chronic hyperkalemia (e.g., hyperkalemia due to CKD or drug-induced hyperkalemia), as opposed to acute hyperkalemia (e.g., due to tissue lysis).

## Information sources

Three sources of information informed parameterization of the  $K^+$  homeostasis model: (1) in vitro  $K^+$ -SZC

binding experiments to initially estimate  $K^+$ -SZC binding affinity,<sup>13</sup> (2) individual patient-level  $sK^+$  data from two phase III trials of SZC to fit all rate constants in the  $K^+$  homeostasis model for each individual patient,<sup>14,15</sup> and (3) established literature knowledge about  $K^+$  homeostasis to constrain model parameters, compartment volumes, and transfer rates to plausible physiological ranges.<sup>19</sup> An overview of the model development process and the clinical trial datasets used for model development is shown in Figure 2, and the physiological constraints are summarized in the top left inset in Figure 1.

Dosing record information in the two clinical trials used to fit the model, ZS-003 (NCT01737697)<sup>15</sup> and ZS-004 (NCT02088073),<sup>14</sup> allowed for explicit modeling of individual patients' dosing regimens in simulations, including deviations from protocol and trial dropout. Conversely, no information on  $K^+$  intake was available from these studies. Lacking such information,  $K^+$  consumption was assumed to be 100 mEq/day for all subjects, with 25% consumed at 8 AM for breakfast, 33% at noon for lunch, and 42% at 6 PM for dinner.

**TABLE 1** Model parameters.

Parameter	Description	Units	Lower bound	Upper bound	Distribution of estimated values [median (IQR)]
$r_{\text{on}}$	$\text{K}^+$ binding to SZC	$\text{mM}^{-1}\text{h}^{-1}$	–	–	Fit to in vitro data (Figure S2), then tuned. Same for all subjects
$r_{\text{off}}$	$\text{K}^+$ unbinding from SZC	$\text{h}^{-1}$	–	–	Fit to in vitro data (Figure S2). Same for all subjects
$r_{\text{GB}}$	$\text{K}^+$ transport GI to blood	$\text{h}^{-1}$	0.005	10	0.062 (0.041, 0.11)
$r_{\text{BG}}$	$\text{K}^+$ transport blood to GI	$\text{h}^{-1}$	0.01	20	0.23 (0.09, 3.8)
$r_{\text{BE}}$	$\text{K}^+$ transport blood to tissue extracellular fluid	$\text{h}^{-1}$	–	–	Fixed: $r_{\text{BE}} = 2.3 * r_{\text{EB}}$ (volume ratio)
$r_{\text{EB}}$	$\text{K}^+$ transport tissue extracellular fluid to blood	$\text{h}^{-1}$	0.008	50	3.9 (0.14, 49.9)
$r_{\text{EI}}$	$\text{K}^+$ uptake by cells in tissue	$\text{h}^{-1}$	0.03	10	0.091 (0.069, 0.12)
$r_{\text{IE}}$	$\text{K}^+$ release by cells in tissue	$\text{h}^{-1}$	0.0001	0.2	0.0011 (0.00083, 0.0015)
$r_{\text{CL,K}}$	$\text{K}^+$ clearance, GI (feces)	$\text{h}^{-1}$	0.0001	0.12	0.0065 (0.0036, 0.011)
$r_{\text{CL,SZC}}$	SZC and $\text{K}^+$ -SZC clearance, GI (feces)	$\text{h}^{-1}$	0.01	15	0.42 (0.26, 0.79)
$r_{\text{renal}}$	Renal $\text{K}^+$ clearance from blood	$\text{h}^{-1}$	0.01	1	0.18 (0.13, 0.29)
$p$	Magnitude of diurnal variation in renal $\text{K}^+$ clearance rate	None	0	1	0.20 (0.073, 0.49)

Note:  $r$  used to denote rates instead of  $K$  to avoid confusion with potassium ( $\text{K}^+$ ).

Abbreviations: GI, gastrointestinal; IQR, interquartile range;  $\text{K}^+$ , potassium;  $\text{sK}^+$ , serum potassium; SZC, sodium zirconium cyclosilicate.

## $\text{K}^+$ -SZC binding rate estimation

The binding and unbinding rates for  $\text{K}^+$  to SZC were initially fit to in vitro data measuring time-course  $\text{K}^+$ -ZS-9 (protonated form of SZC) binding at three different pH levels (to mimic the stomach, small intestine, and large intestine environments).<sup>13</sup> The ZS-9 batch used in this experiment had a  $\text{K}^+$  exchange capacity about 70% that of the batches used in ZS-003 and ZS-004. The binding and unbinding rates fit to the small intestine-matched pH experiment were used as an initial estimate in the  $\text{K}^+$ -SZC/free- $\text{K}^+$  homeostasis model (Figure S2) and were assumed to be the same for all subjects.

## Individual patient $\text{K}^+$ homeostasis parameter estimation

The nine remaining model parameters (summarized in Table 1) were optimized separately for each patient, minimizing the least squared error between patient  $\text{sK}^+$  data and simulations, with the addition of penalties to ensure a physiological  $\text{K}^+$  distribution. Individual parameter sets were fit one at a time, instead of using a population-based approach, because the expected distributions for many parameters were unknown, dosing regimens were different for each participant, and good capture of  $\text{sK}^+$  over time was desired for each participant, not just at

the population level. This approach allowed for capture of subject-to-subject differences due to covariates that were not measured and is well-suited to predict scenarios not tested in the clinic, as opposed to determining the effect size of specific covariates. Parameters were fit using the robust local Levenberg–Marquardt algorithm, with upper and lower parameter bounds specified to prevent solver errors (Table 1). To improve the probability of obtaining a good fit for each patient, the solver was run 12 times for each subject with different initial parameter guesses.

Prior physiological knowledge about  $\text{K}^+$  homeostasis, as summarized in Figure 1, was introduced into the model in the form of penalties added to the cost function. For these constraints, baseline  $\text{sK}^+$  values were evaluated at midnight before the first dose or over a 24-h period without SZC, as appropriate, with the model at steady-state. These conditions were not strictly enforced; they could be slightly violated if the fit improved sufficiently to decrease overall cost. In the absence of reliable measurements, GI  $\text{K}^+$  was not constrained. Additionally, a 50% higher weight was given to  $\text{sK}^+$  measurements in the first 48 h, to improve capture of baseline  $\text{sK}^+$  levels and the dynamic time-course response to t.i.d. SZC dosing.

Due to the constraint that baseline plasma and tissue extracellular  $\text{K}^+$  equilibrate quickly, the ratio of the respective forward and reverse rates was always approximately equal to the ratio of the respective compartment

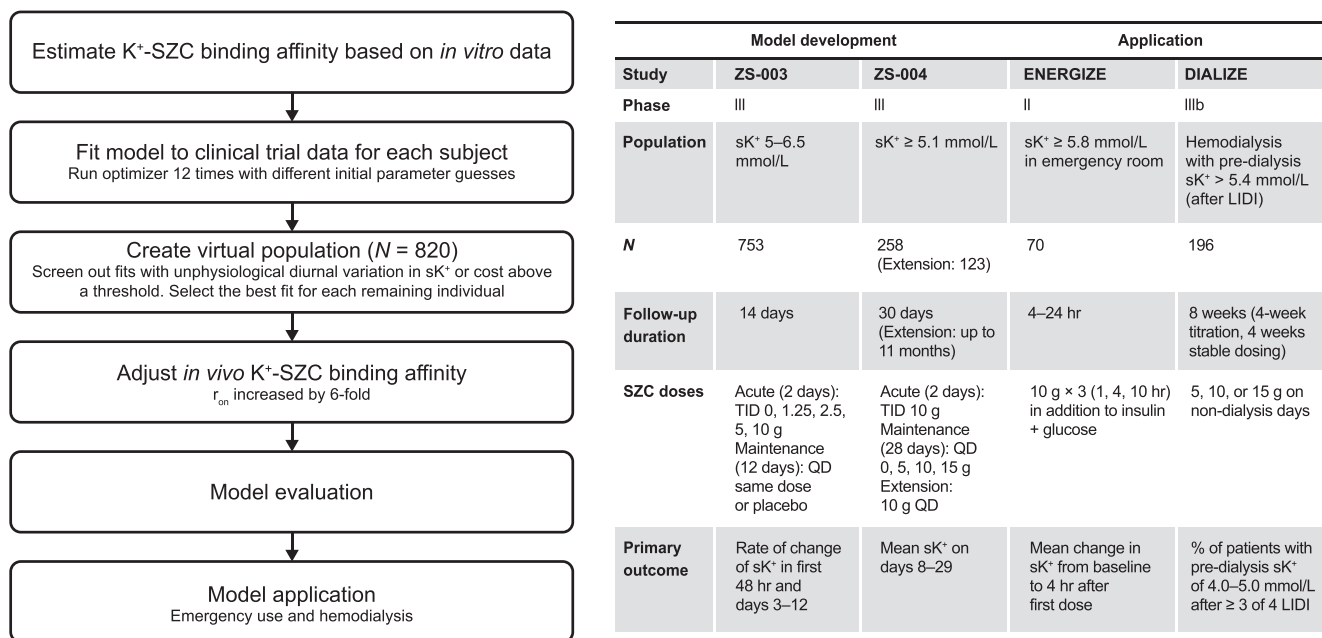


**FIGURE 2** Overview of model development and clinical data used in this analysis. Left: Flow chart of the model development process. Right: Summary of datasets used to develop the model, and to which the model was applied.  $K^+$ , potassium; LIDI, long interdialytic interval; QD, once per day dosing;  $r_{on}$ , rate of  $K^+$ -SZC binding;  $sK^+$ , serum potassium; SZC, sodium zirconium cyclosilicate; TID, three times per day dosing.

volumes. Therefore,  $r_{EB}$  was estimated and  $r_{BE}$  was set to  $r_{BE} = 2.3 \times r_{EB}$ .

## Virtual population creation

After running the optimization routine 12 times for each patient, fits with diurnal variation in  $sK^+$  less than 1.7% or greater than 15% were screened out, as were fits with unacceptably high cost (threshold based on visual inspection as  $0.7 \times$  length of residuals). These steps ensured exclusion of poor and/or unphysiological parameter sets in the virtual population. The remaining parameter set with the lowest cost for each subject was selected, resulting in accepted fits for 652 (87%) patients from ZS-003 and 168 (65%) patients from ZS-004, for a virtual population of 820 subjects, which is summarized in Table S2.

## Model evaluation and tuning of *in vivo* $K^+$ -SZC binding

To evaluate model performance, simulated  $sK^+$  time-course data were compared graphically to observed trial data for each arm of ZS-003 and ZS-004 (shown for ZS-004 in Figure S2). Based upon this analysis, which showed an underestimation of reduction in  $sK^+$  following SZC dosing, the rate of  $K^+$ -SZC binding ( $r_{on}$ ) was increased by a factor of six to better match the observed clinical trial data;

binding is fast relative to the timescales in the clinical studies, so the implications of changing  $r_{on}$  versus  $r_{off}$  are minimal. The difference in *in vitro* and estimated clinical binding affinity may be due to differences in pH and other conditions, as well as use of an earlier, protonated form of SZC (ZS-9), in the *in vitro* experiment.

## Model application to inform trial design and decision making

The virtual population was used to inform internal decision making for trials of SZC in novel applications: reduction of  $sK^+$  in an emergency setting and prevention of hyperkalemia in a hemodialysis population. In each case, the renal clearance of  $K^+$  was adjusted to match the simulated population  $sK^+$  to the target population, and then the virtual population was subset to match trial inclusion criteria (summarized in Figure 2). Each proposed SZC dosing regimen was applied to each virtual subject. For reproducibility, the means and covariance matrix of all parameters, eGFR, and body weight for the virtual population, as well as a template simulation script, are included in File S1.

## Software details

*In vitro* binding constants were estimated in Microsoft Excel. All other model estimation was done in R 3.3.0,

and all simulation and plotting were performed in R 4.0.2. The set of differential equations were solved using the Livermore Solver for Ordinary Differential Equations with adaptive method switching for stiff and non-stiff systems in the deSolve package. Run-time for a single subject is on the order of seconds. Parameters fitting was done with minpack.lm, implemented via the FME package.

## RESULTS

### Model development and evaluation

The SZC-K<sup>+</sup> homeostasis model is composed of four compartments to describe K<sup>+</sup> intake, distribution, and elimination, as well as patient-specific dosing of SZC and binding of K<sup>+</sup> and SZC in the GI tract (Figure 1). Physiological constraints were incorporated while fitting the model to ensure reasonable behavior for each individually fit patient in the resulting virtual population. The overall model performance across subjects was inspected graphically to ensure appropriate capture of central tendencies and variability in K<sup>+</sup> dynamics and SZC dose-response.

Plots of sK<sup>+</sup> over time in each arm of ZS-003 with SZC doses greater than 2.5 g, and all arms of ZS-004 are shown in Figure 3. Overall, model performance was acceptable for acute t.i.d. SZC treatment, maintenance q.d. SZC treatment, and follow-up after cessation of SZC treatment. In some cases, patients treated with placebo did not return to their baseline sK<sup>+</sup> levels, as the simulated subjects did, leading to imperfect fits in some placebo and low dose arms (Figure 3, Figures S3 and S4). However, both the mean and variability were reasonably well-captured. Examination of observed versus predicted sK<sup>+</sup> (Figures S3 and S4) showed some under-prediction of the most extreme (high and low) sK<sup>+</sup> values. This was not unexpected, given the limited detail in this model on the nonlinear regulatory mechanisms involved in K<sup>+</sup> homeostasis, as well as the lack of data on actual K<sup>+</sup> intake. As such, the model performance was deemed acceptable for the intended purpose of informing trial design for SZC in new applications.

### Treatment of severe hyperkalemia in an emergency setting with SZC

As severe hyperkalemia elevates the risk of life-threatening cardiac arrhythmias and death, it is critical to reduce sK<sup>+</sup> as quickly as possible.<sup>22</sup> Current standard of care involves co-administration of insulin and glucose to induce insulin-mediated cellular uptake of K<sup>+</sup> without hypoglycemia,<sup>23</sup> followed as needed by dialysis. A phase II trial was planned to test the ability of SZC to improve on

emergency management of severe hyperkalemia.<sup>22</sup> The highest dose of SZC that had been studied at that time was 10 g t.i.d. The SZC-K<sup>+</sup> homeostasis model was used to predict whether this dosing regimen would be sufficient or whether higher SZC doses would be required to lower sK<sup>+</sup> sufficiently and quickly enough.

The simulations performed to address this question are summarized in Figure 4. First, the baseline sK<sup>+</sup> of the virtual population was adjusted, and the population was subset to match the target population for the trial. In simulations, it was assumed that subjects arrived in the emergency department at 8 PM for the baseline sK<sup>+</sup> measurement, a time of day when sK<sup>+</sup> levels are predicted to be relatively high. The simulated SZC dosing regimens were: 10 g given three times (1, 4, and 10 h post-baseline), 30 g given once (at 1 h post-baseline), and 60 g given once (at 1 h post-baseline). Note that the virtual subjects had chronic hyperkalemia, whereas actual subjects would likely arrive in the emergency department with higher than their typical sK<sup>+</sup> levels. The primary trial end point was reduction in sK<sup>+</sup> to below 5.5 mmol/L within 4 h post-baseline (Figure 2). The simulations predicted that 10 g SZC would produce very modest changes in sK<sup>+</sup> within 4 h, and that 30 g SZC was also not sufficient for the average subject to achieve sK<sup>+</sup> less than 5.5 mmol/L within 4 h. However, 60 g SZC was predicted to be sufficient (Figure 4).

As this SZC dose would be notably higher than any doses in clinical trials to date, these simulations contributed to a decision to test SZC 10 g × 3 on top of treatment with insulin + glucose, instead of alone, in the phase II ENERGIZE trial (NCT03337477). This trial has now been completed, and consistent with simulations, SZC 10 g × 3 treatment did not significantly reduce sK<sup>+</sup> within 4 h in the treated population.<sup>22</sup>

### SZC to control sK<sup>+</sup> in hemodialysis patients

Hemodialysis is typically performed three times per week in patients with end-stage renal disease.<sup>24,25</sup> Whereas dialysis removes excess K<sup>+</sup> from the blood, particularly with use of a low-K<sup>+</sup> dialysate, hyperkalemia is a common complication in these patients, particularly over the 3-day long interdialytic interval (LIDI).<sup>24,26</sup> This pre-dialysis hyperkalemia after the LIDI is associated with an increased risk of sudden cardiac arrest and death.<sup>27</sup> As such, a trial (DIALIZE, NCT03303521) was designed to test whether SZC administration on non-dialysis days could help hemodialysis patients maintain normokalemia between dialysis treatments.<sup>28</sup> The SZC-K<sup>+</sup> model was applied to determine whether SZC was likely to be effective in this application, and what SZC dose range would be appropriate to study (Figure 5).

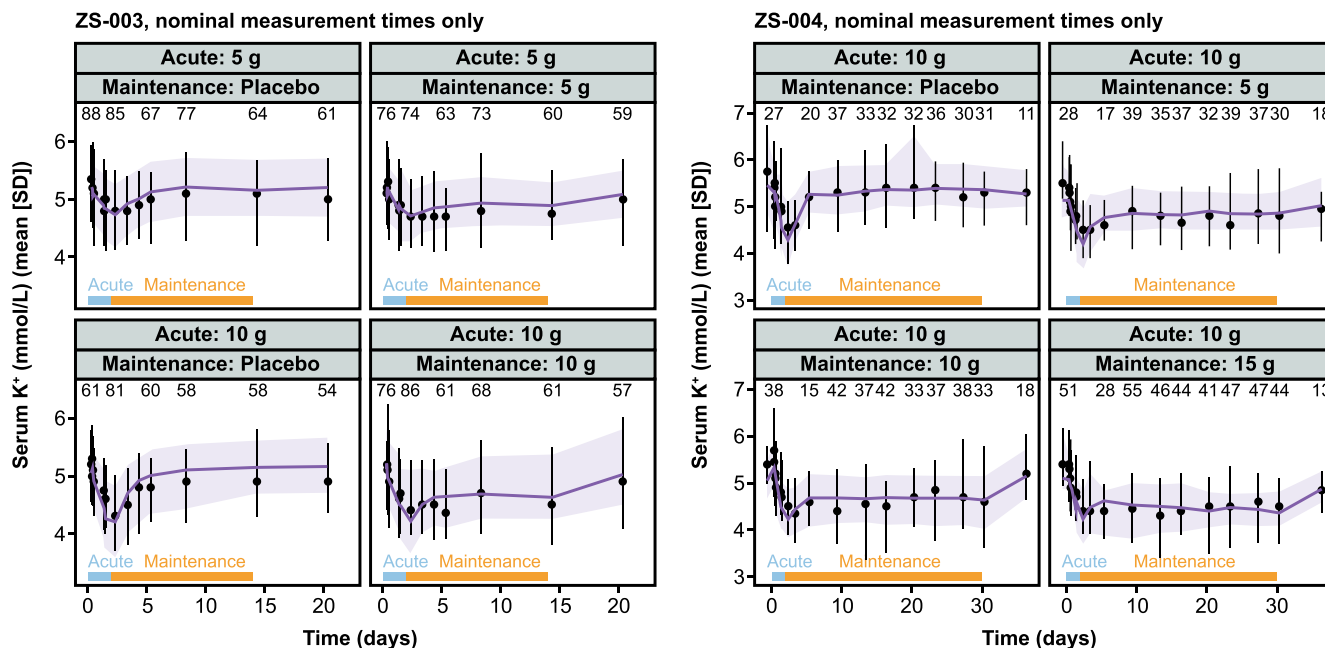


**FIGURE 3** Comparison of data and model predictions by study arm. Left: SZC-003 arms with SZC doses greater than 2.5 g. Right: SZC-004. Purple lines and ribbon are simulations, black lines, points, and error bars are study data. Blue bars show acute (three times per day) dosing, and orange bars show maintenance (once per day) dosing periods. Simulated data are shown only at timepoints with available clinical data for clarity, and low-dose arms from SZC-003 are omitted. Plots with all simulated timepoints and all trial arms can be found in the Appendix S1, along with plots of individual observed versus predicted  $sK^+$  data points. Lines are means and shaded bands and error bars are mean  $\pm$  SD. Numbers are the number of  $sK^+$  measurements available at each timepoint. Data from Stavros et al. and Kosiborod et al.<sup>14,15</sup>  $K^+$ , potassium; SD, standard deviation;  $sK^+$ , serum potassium; SZC, sodium zirconium cyclosilicate.

Hemodialysis was incorporated into the model by addition of a “dialysis bath” compartment (Figure 1), with a one-way transfer of  $K^+$  from the blood to this fixed [ $K^+$ ] compartment, which could be turned on during simulated hemodialysis sessions. At the time, data from an observational study<sup>29</sup> of  $sK^+$  in hemodialysis patients were used to specify the dialysate  $K^+$ , duration of dialysis, and rate of  $K^+$  transfer from blood to the dialysate ( $r_D$ ). As the SZC trial DIALIZE is now completed, we show here tuning of the model to match dialysis parameters from the placebo arm of this trial.<sup>28</sup> The virtual population was subset to subjects with eGFR less than 20 mL/min/1.73 m<sup>2</sup>, and dialysis was implemented on a Monday–Wednesday–Friday schedule for 4 h starting at 8 AM, with a dialysate  $K^+$  of 2 mmol/L, aligned with median parameters in the DIALIZE trial.<sup>28</sup> The baseline  $sK^+$  in the virtual population was adjusted to match the pre-dialysis levels in DIALIZE, and the  $K^+$  transfer rate  $r_D$  was then tuned to capture the placebo arm post-dialysis  $sK^+$  in DIALIZE (Figure 5, top right).

With no additional tuning, the model was then used to predict  $sK^+$  dynamics in hemodialysis patients treated with 5, 10, or 15 g SZC once daily on non-dialysis days. The trial involved a 4-week SZC dose titration, followed by a 4-week stable dose evaluation period (Figure 2). In simulations, it was assumed that the dose would

increase by one step each week until the target dose was reached. During the stable treatment period, seven subjects were on SZC 0 g, 33 subjects on 5 g, 39 subjects on 10 g, and 17 subjects on 15 g. As shown in Figure 5 (right middle), the predictions accorded well with the observed data from DIALIZE for the pre- and post-dialysis  $sK^+$  after the last LIDI in the evaluation period; the observed data for subjects treated with SZC were similar to the simulated pre-dialysis  $sK^+$  with SZC 15 g, and the post-dialysis  $sK^+$  with SZC 10 g. Although this represents somewhat of an underprediction of the observed SZC response, the predictions were quite reasonable considering the extrapolation to a new population, and the relatively simple implementation of hemodialysis in the model. The population variability in  $sK^+$  was also well matched to observed data, suggesting the modifications to the virtual population captured the  $sK^+$  range in hemodialysis patients well. The model predicted a relatively linear dose–response (Figure 5), something that could not be easily evaluated in the clinical trial due to the dose titration. Additionally, simulations predicted that a SZC once-daily dose of 15 g would be sufficient to prevent progressive increases in the daily  $sK^+$  peak during the LIDI, and to maintain peak  $sK^+$  below 5.5 mmol/L for the average patient, with minimal risk of  $sK^+$  falling below 3 mmol/L (Figure 5, bottom right).



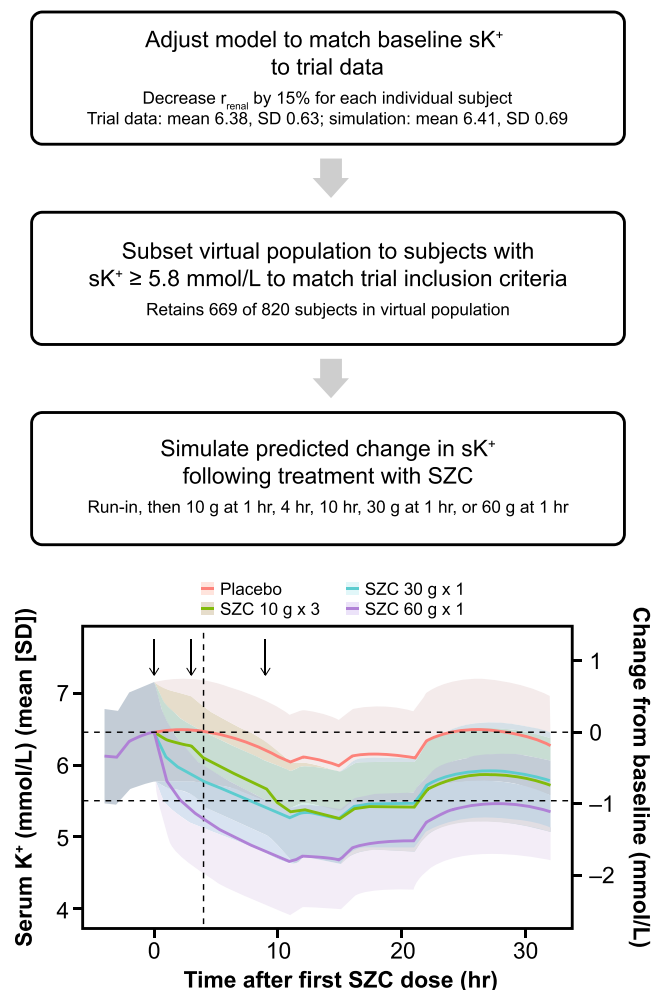


**FIGURE 4** Model application to SZC dosing in emergency settings. Top: Flow chart of process to adjust model to simulate severe hyperkalemia to mimic desired trial population and simulate different SZC dosing regimens. Bottom: Predicted  $sK^+$  following examined SZC dosing regimens. Horizontal dashed lines are baseline  $sK^+$  and the upper limit of normal (5.5 mmol/L), the vertical dashed line is 4 h post-baseline (time of primary end point), and the black arrows denote times of SZC doses. Lines are means and shaded bands are means  $\pm$  SD.  $K^+$ , potassium; SD, standard deviation;  $r_{\text{renal}}$ , renal  $K^+$  clearance from blood;  $sK^+$ , serum potassium; SZC, sodium zirconium cyclosilicate.

The predictions of SZC response in hemodialysis patients were used to provide confidence in the probability of success of the DIALIZE trial, to determine appropriate SZC doses to test in the clinical trial, and inform the decision to dose SZC on non-dialysis days as opposed to every day, in order to minimize the risk of hypokalemia (Figure S5).

## DISCUSSION

This analysis developed and applied a model of  $K^+$  homeostasis and SZC pharmacodynamics to inform design

of clinical trials in emergency treatment of severe hyperkalemia and in hemodialysis patients. The model was fit-for-purpose, with sufficient physiological detail to capture trends and variability in  $K^+$  distribution and transport, but simple enough to be fit to the available clinical data. Overall, the model achieved these objectives; the performance was sufficient to capture overall population behavior in the two trials to which the model was fit. Additionally, with first principles – based modifications to the virtual population (increasing baseline  $sK^+$  and a relatively simple implementation of dialysis), the model successfully captured  $sK^+$  over time in a hemodialysis population and predicted the SZC dose–response in the population reasonably well, despite inclusion of limited mechanistic detail on CKD and regulation of  $K^+$  by insulin, as well as the differences in these settings compared to the trials to which the model was fit.

In emergency lowering of  $sK^+$ , the model predicted that higher doses of SZC than had previously been tested in clinical studies would be required to normalize  $sK^+$  fast enough to meet treatment goals, a prediction that was borne out in the final results of the ENERGIZE trial.<sup>22</sup> Whereas this was a “negative” example, it is still a case where the model brought valuable insight during decision making. Importantly, this model demonstrates the value of fit-for-purpose systems physiology models both after initial approval of a drug, when there are still many unknowns and new applications that modeling can inform, and when more clinical data are available upon which to construct a model.

Although this model was sufficient to inform the development program for expansion of SZC into new applications,  $K^+$  homeostasis is also important in other applications, including optimizing RAASi treatment in CKD and heart failure.<sup>1,11</sup> As such, this model could be used to further study aspects of  $K^+$  homeostasis that are difficult to measure experimentally without radiolabeled tracer studies, such as how the distribution of  $K^+$  shifts with disease-related changes, as well as treatment with different  $K^+$  binders. Another interesting avenue is variation in  $sK^+$  over the course of the day, as a function of diurnal variation, and meal and SZC dose timing. Many times, clinical trial measurements are made before the first meal in the morning, at which time  $sK^+$  levels are near their lowest for the day, and therefore least likely to be above the normal range.<sup>6,7</sup>

The model currently includes limited physiological detail (e.g., GI compartments) and limited detail on the complexity of  $K^+$  regulation; this could be expanded upon in the future using information from literature based on detailed physiological experiments and data from large trials of drugs that influence  $K^+$  handling (e.g., aldosterone antagonists), as explored by Stadt et al.<sup>18</sup> and Maddah and

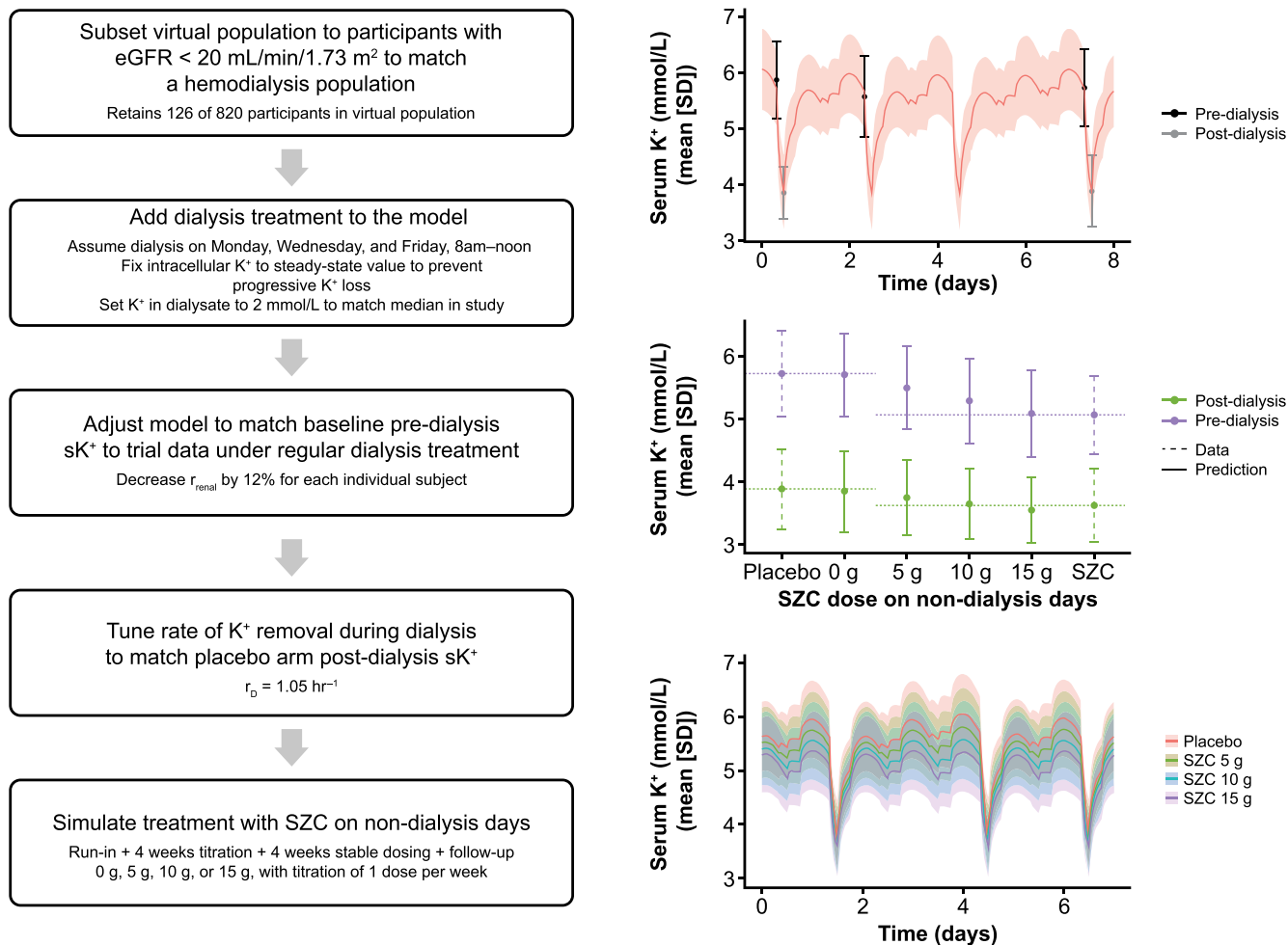


**FIGURE 5** Model application to SZC dosing in hemodialysis. Left: Flow chart of process to adjust model to simulate dialysis, tune model to match target population, and simulate different SZC dosing regimens. Top right: Placebo arm data (days 50–58; last week of evaluation period) from DIALIZE and simulated  $sK^+$  after tuning of baseline  $sK^+$  and dialysis  $K^+$  removal rate to match clinical data. Middle right: Pre- and post-dialysis  $sK^+$  in DIALIZE (dashed error bars)<sup>28</sup> and each simulated SZC dosing group (solid error bars) after the last LIDI of the evaluation period. Bottom right: SZC dose-response of  $sK^+$  over a representative week of stable dosing, with the SZC dose given at 8 AM each dosing day. Note that with SZC 15 g on non-dialysis days, peak daily  $sK^+$  no longer increased substantially over the LIDI (days 2–4). Lines are means and shaded bands and error bars are means  $\pm$  SD. eGFR, estimated glomerular filtration rate;  $K^+$ , potassium;  $r_D$ , rate of  $K^+$  transfer; LIDI, long interdialytic interval;  $r_{\text{renal}}$ , renal  $K^+$  clearance from blood; SD, standard deviation;  $sK^+$ , serum potassium; SZC, sodium zirconium cyclosilicate.

Hallow.<sup>17</sup> Such refinement would improve the fidelity of the model in capturing  $sK^+$  trends at the highest and lowest ends, where underlying regulatory systems are likely not working optimally. For example, in late CKD, more  $K^+$  is cleared via the GI tract due to reduced kidney function.<sup>8,30</sup> The effects of increased blood pressure, changes in volumes due to edema, prescription of a low- $K^+$  diet, changes to the function of the RAAS system, and the effects of different classes of diuretics and RAASi could also be modeled in much more detail.<sup>4,31</sup> Similarly, in diabetes, insulin resistance can affect the ability of cells to uptake  $K^+$  quickly in an insulin-dependent manner, reducing the ability to buffer changes in tissue extracellular  $K^+$ .<sup>1,5</sup> There is also evidence of GI-kidney crosstalk in  $K^+$  regulation:

oral  $K^+$  alone, oral  $K^+$  as part of a complex meal, and intravenous  $K^+$  lead to different changes in renal  $K^+$  excretion that cannot be explained by the actions of aldosterone alone.<sup>32–34</sup> Although  $K^+$  regulation is complex, and further mechanistic detail would likely improve the applicability of this model to extrapolate to additional patient populations and scenarios, this model provides a solid groundwork for further exploration and systems-level understanding of  $K^+$  homeostasis, dysregulation in disease, and changes with SZC treatment.

#### AUTHOR CONTRIBUTIONS

L.E.C. wrote the manuscript. L.E.C., L.C., M.N., D.W.B., and R.C.P. designed the research. L.E.C. and L.C.

performed the research. L.E.C., L.C., M.N., D.W.B., and R.C.P. analyzed the data. L.E.C. and L.C. contributed new reagents/analytical tools.

## ACKNOWLEDGMENTS

Editorial and submission support, funded by AstraZeneca, was provided by Melissa Ward, BA of Core, London, UK, in accordance with Good Publication Practice guidelines.

## FUNDING INFORMATION

This study was funded by AstraZeneca.

## CONFLICT OF INTEREST STATEMENT

L.E.C., M.N., D.W.B., and R.C.P. are current shareholders and/or employees of AstraZeneca. L.C. was an employee of AstraZeneca when this work was performed.

## DATA AVAILABILITY STATEMENT

Data underlying the findings described in this manuscript may be obtained in accordance with AstraZeneca's data sharing policy described at <https://astrazenecagrouptrials.pharmacm.com/ST/Submission/Disclosure>. Data for studies directly listed on Vivli can be requested through Vivli at [www.vivli.org](http://www.vivli.org). Data for studies not listed on Vivli could be requested through Vivli at <https://vivli.org/members/enquiries-about-studies-not-listed-on-the-vivli-platform/>. AstraZeneca Vivli member page is also available outlining further details: <https://vivli.org/ourmember/astrazeneca/>. In order to simulate virtual patients with the model presented in this paper, the means and a covariance matrix of the individual parameters and covariates used in this analysis are provided in the Appendix S1, along with an R script that can generate virtual patients and perform simulations.

## ORCID

Lindsay E. Clegg  <https://orcid.org/0000-0001-8558-9341>

Mats Nagard  <https://orcid.org/0000-0001-9643-1638>

David W. Boulton  <https://orcid.org/0000-0002-0668-7304>

Robert C. Penland  <https://orcid.org/0000-0003-2706-8913>

## REFERENCES

- Hunter RW, Bailey MA. Hyperkalemia: pathophysiology, risk factors and consequences. *Nephrol Dial Transplant*. 2019;34:iii2-iii11. doi:10.1093/ndt/gfz206
- Rabelink TJ, Koomans HA, Hené RJ, Dorhout Mees EJ. Early and late adjustment to potassium loading in humans. *Kidney Int*. 1990;38:942-947. doi:10.1038/ki.1990.295
- Kovesdy CP, Matsushita K, Sang Y, et al. Serum potassium and adverse outcomes across the range of kidney function: a CKD prognosis consortium meta-analysis. *Eur Heart J*. 2018;39:1535-1542. doi:10.1093/eurheartj/ehy100
- Palmer BF, Clegg DJ. Physiology and pathophysiology of potassium homeostasis. *Adv Physiol Educ*. 2016;40:480-490. doi:10.1152/advan.00121.2016
- Gumz ML, Rabinowitz L, Wingo CS. An integrated view of potassium homeostasis. *N Engl J Med*. 2015;373:60-72. doi:10.1056/NEJMra1313341
- Moore-Ede MC, Herd JA. Renal electrolyte circadian rhythms: independence from feeding and activity patterns. *Am J Physiol*. 1977;232:F128-F135. doi:10.1152/ajprenal.1977.232.2.F128
- Moore-Ede MC, Meguid MM, Fitzpatrick GF, Boyden CM, Ball MR. Circadian variation in response to potassium infusion. *Clin Pharmacol Ther*. 1978;23:218-227. doi:10.1002/cpt1978232218
- Bastl C, Hayslett JP, Binder HJ. Increased large intestinal secretion of potassium in renal insufficiency. *Kidney Int*. 1977;12:9-16. doi:10.1038/ki.1977.73
- Ueda Y, Ookawara S, Ito K, et al. Changes in urinary potassium excretion in patients with chronic kidney disease. *Kidney Res Clin Pract*. 2016;35:78-83. doi:10.1016/j.krcp.2016.02.001
- Parving H-H, Brenner BM, McMurray JJV, et al. Cardiorenal end points in a trial of Aliskiren for type 2 diabetes. *N Engl J Med*. 2012;367:2204-2213. doi:10.1056/NEJMoa1208799
- Chin KL, Skiba M, Tonkin A, et al. The treatment gap in patients with chronic systolic heart failure: a systematic review of evidence-based prescribing in practice. *Heart Fail Rev*. 2016;21:675-697. doi:10.1007/s10741-016-9575-2
- Palmer BF. Potassium binders for hyperkalemia in chronic kidney disease-diet, renin-angiotensin-aldosterone system inhibitor therapy, and hemodialysis. *Mayo Clin Proc*. 2020;95:339-354. doi:10.1016/j.mayocp.2019.05.019
- Stavros F, Yang A, Leon A, Nuttall M, Rasmussen HS. Characterization of structure and function of ZS-9, a K<sup>+</sup> selective ion trap. *PLoS One*. 2014;9:e114686. doi:10.1371/journal.pone.0114686
- Kosiborod M, Rasmussen HS, Lavin P, et al. Effect of sodium zirconium cyclosilicate on potassium lowering for 28 days among outpatients with hyperkalemia: the HARMONIZE randomized clinical trial. *Jama*. 2014;312:2223-2233. doi:10.1001/jama.2014.15688
- Packham DK, Rasmussen HS, Lavin PT, et al. Sodium zirconium cyclosilicate in hyperkalemia. *N Engl J Med*. 2014;372:222-231. doi:10.1056/NEJMoa1411487
- Ash SR, Singh B, Lavin PT, Stavros F, Rasmussen HS. A phase 2 study on the treatment of hyperkalemia in patients with chronic kidney disease suggests that the selective potassium trap, ZS-9, is safe and efficient. *Kidney Int*. 2015;88:404-411. doi:10.1038/ki.2014.382
- Maddah E, Hallow KM. A quantitative systems pharmacology model of plasma potassium regulation by the kidney and aldosterone. *J Pharmacokinet Pharmacodyn*. 2022;49:471-486. doi:10.1007/s10928-022-09815-x
- Stadt MM, Leete J, Devinyak S, Layton AT. A mathematical model of potassium homeostasis: effect of feedforward and feedback controls. *PLoS Comput Biol*. 2022;18:e1010607. doi:10.1371/journal.pcbi.1010607
- Boron WF, Boulpaep EL. *Medical Physiology: A Cellular and Molecular Approach*, Updated Edition. Elsevier Saunders; 2005.

20. Mudie DM, Murray K, Hoad CL, et al. Quantification of gastrointestinal liquid volumes and distribution following a 240 mL dose of water in the fasted state. *Mol Pharm*. 2014;11:3039-3047. doi:[10.1021/mp500210c](https://doi.org/10.1021/mp500210c)
21. Schiller C, Fröhlich CP, Giessmann T, et al. Intestinal fluid volumes and transit of dosage forms as assessed by magnetic resonance imaging. *Aliment Pharmacol Ther*. 2005;22:971-979. doi:[10.1111/j.1365-2036.2005.02683.x](https://doi.org/10.1111/j.1365-2036.2005.02683.x)
22. Peacock WF, Rafique Z, Vishnevskiy K, et al. Emergency potassium normalization treatment including sodium zirconium cyclosilicate: a phase II, randomized, double-blind, placebo-controlled study (ENERGIZE). *Acad Emerg Med*. 2020;27:475-486. doi:[10.1111/acem.13954](https://doi.org/10.1111/acem.13954)
23. Peacock WF, Rafique Z, Clark CL, et al. Real world evidence for treatment of hyperkalemia in the emergency department (REVEAL-ED): a multicenter, prospective, observational study. *J Emerg Med*. 2018;55:741-750. doi:[10.1016/j.jemermed.2018.09.007](https://doi.org/10.1016/j.jemermed.2018.09.007)
24. Brunelli SM, Du Mond C, Oestreicher N, Rakov V, Spiegel DM. Serum potassium and short-term clinical outcomes among hemodialysis patients: impact of the long interdialytic interval. *Am J Kidney Dis*. 2017;70:21-29. doi:[10.1053/j.ajkd.2016.10.024](https://doi.org/10.1053/j.ajkd.2016.10.024)
25. Karaboyas A, Zee J, Brunelli SM, et al. Dialysate potassium, serum potassium, mortality, and arrhythmia events in hemodialysis: results from the Dialysis Outcomes and Practice Patterns Study (DOPPS). *Am J Kidney Dis*. 2017;69:266-277. doi:[10.1053/j.ajkd.2016.09.015](https://doi.org/10.1053/j.ajkd.2016.09.015)
26. Rhee CM. Serum potassium and the long interdialytic interval: minding the gap. *Am J Kidney Dis*. 2017;70:4-7. doi:[10.1053/j.ajkd.2017.04.007](https://doi.org/10.1053/j.ajkd.2017.04.007)
27. Bleyer AJ, Russell GB, Satko SG. Sudden and cardiac death rates in hemodialysis patients. *Kidney Int*. 1999;55:1553-1559. doi:[10.1046/j.1523-1755.1999.00391.x](https://doi.org/10.1046/j.1523-1755.1999.00391.x)
28. Fishbane S, Ford M, Fukagawa M, et al. A phase 3b, randomized, double-blind, placebo-controlled study of sodium zirconium cyclosilicate for reducing the incidence of predialysis hyperkalemia. *J Am Soc Nephrol*. 2019;30:1723-1733. doi:[10.1681/asn.2019050450](https://doi.org/10.1681/asn.2019050450)
29. Singh B, Block G, Lerma E. Hyperkalemia and serum potassium variability in patients on hemodialysis. *Am J Kidney Dis*. 2017;69:A3.
30. Musso CG. Potassium metabolism in patients with chronic kidney disease (CKD), part I: patients not on dialysis (stages 3-4). *Int Urol Nephrol*. 2004;36:465-468. doi:[10.1007/s11255-004-6193-z](https://doi.org/10.1007/s11255-004-6193-z)
31. Allon M. Treatment and prevention of hyperkalemia in end-stage renal disease. *Kidney Int*. 1993;43:1197-1209. doi:[10.1038/ki.1993.170](https://doi.org/10.1038/ki.1993.170)
32. Preston RA, Afshartous D, Rodco R, Alonso AB, Garg D. Evidence for a gastrointestinal-renal kaliuretic signaling axis in humans. *Kidney Int*. 2015;88:1383-1391. doi:[10.1038/ki.2015.243](https://doi.org/10.1038/ki.2015.243)
33. Oh KS, Oh YT, Kim SW, Kita T, Kang I, Youn JH. Gut sensing of dietary K<sup>+</sup> intake increases renal K<sup>+</sup> excretion. *Am J Physiol Regul Integr Comp Physiol*. 2011;301:R421-R429. doi:[10.1152/ajpregu.00095.2011](https://doi.org/10.1152/ajpregu.00095.2011)
34. Rabinowitz L, Denham SC, Gunther RA. Aldosterone and postprandial renal excretion of sodium and potassium in sheep. *Am J Physiol*. 1977;233:F213-F216. doi:[10.1152/ajprenal.1977.233.3.F213](https://doi.org/10.1152/ajprenal.1977.233.3.F213)

## SUPPORTING INFORMATION

Additional supporting information can be found online in the Supporting Information section at the end of this article.

**How to cite this article:** Clegg LE, Chu L, Nagard M, Boulton DW, Penland RC. Potassium homeostasis and therapeutic intervention with sodium zirconium cyclosilicate: A model-informed drug development case study. *CPT Pharmacometrics Syst Pharmacol*. 2024;13:296-307. doi:[10.1002/psp4.13084](https://doi.org/10.1002/psp4.13084)